Biochemical and Biophysical Research Communications 437 (2013) 349–354

Contents lists available at SciVerse ScienceDirect

Biochemical and Biophysical Research Communications

journal homepage: www.elsevier.com/locate/ybbrc

Guanine nucleotide exchange in the ribosomal GTPase EFL1 is modulated by the protein mutated in the Shwachman–Diamond Syndrome

Abril Gijsbers, Adrián García-Márquez, Axel Luviano, Nuria Sánchez-Puig *

Departamento de Química de Biomacromoléculas, Instituto de Química, Universidad Nacional Autónoma de México, Av. Universidad 3000, Ciudad Universitaria, C.P. 04510, México, D.F., Mexico

ARTICLE INFO

Article history:
Received 10 June 2013
Available online 4 July 2013

Keywords:
GTPase
Guanine exchange factor
EFL1
Shwachman–Diamond Syndrome protein

ABSTRACT

Ribosome biogenesis in eukaryotes is a complex process that requires the participation of several accessory proteins that are not part of the mature particle. Efl1 is a yeast GTPase required for the cytoplasmic maturation of the 60S ribosomal subunit. Together with Sdo1, the yeast ortholog of the protein mutated in the Shwachman–Diamond Syndrome (SBDS), Efl1 releases the anti-association factor Tif6 from the surface of the 60S subunit allowing the assembly of mature ribosomes. We characterized the structural content and folding stability of the *Saccharomyces cerevisiae* and human EFL1 GTPases, as well as their enzymatic properties alone and in the presence of Sdo1 and SBDS, respectively. The human and *S. cerevisiae* EFL1 GTPases are composed of a mixture of α-helices and β-sheets. Despite being orthologs, the yeast protein elicited a non-two state thermal unfolding behavior while the human EFL1 was highly resistant to thermal denaturation. Steady-state kinetic analyses indicated slow GTP hydrolysis for both EFL1 GTPases, with k_{cat} values of 0.4 and 0.3 min^{-1} and K_m for GTP of 110 and 180 μM respectively. In the presence of the effector proteins, their k_{cat} values remained unaltered while the K_m decreased twofold suggesting that Sdo1 and SBDS act as nucleotide exchange factors.

1. Introduction

Ribosomes are the molecular machines responsible for the synthesis of proteins. To synthesize proteins, it is necessary to first synthesize ribosomes. In eukaryotes, ribosome biogenesis requires the coordinated assembly of four ribosomal RNAs and nearly 80 ribosomal proteins aided by approximately 200 assembly proteins that are not part of the mature ribosome structure [1–3]. In *Saccharomyces cerevisiae*, 20% of these assembly factors are associated to nucleoside triphosphate hydrolyzing enzymes such as GTPases, ATPases and kinases [4]. GTPases comprise one of the largest class of essential ribosome assembly factors in living organisms [5,6]. Yeast ribosome biogenesis requires the activity of six GTPases: Bms1 for assembly of the 40S subunit [7] and Nog1, Nog2, Nug1, Lsg1 and Efl1 for assembly of the 60S subunit [8–12]. The last two cytoplasmic maturation steps of the 60S subunit are mediated by the GTPases Lsg1 and Efl1. The GTPase activity of Efl1 is coupled by the Sdo1 protein (the yeast ortholog mutated in the Shwachman–Bodian–Diamond Syndrome, SBDS) to release Tif6 from the surface of the 60S subunit [11,13]. Tif6 binds to the 60S intersubunit bridge B6 and prevents premature association of the ribosomal subunits [14]. Efl1 is also involved in a checkpoint that tests the functionality of the 60S ribosomal subunits before they enter the pool of translating ribosomes. Efl1 is homologous to the ribosomal translocases EF-G/EF-2 and binds the 60S subunit in the GTPase-associated center (GAC) [15,16]. In a translation-like step similar to that mediated by EF-2 during mRNA–tRNA translocation, Efl1 assess the correct assembly of the ribosome stalk and a loop of Rpl10 located in the P-site triggering a GTPase-dependent conformational change that releases Tif6 [17,18].

Amongst the proteins that bind and hydrolyze nucleoside triphosphates; GTPases belong to the P-loop GTPase fold. GTPases can be classified into two large classes designated as the TRAFAC (for translation factor-related) and the SIMIBI class [19]. The TRAFAC class comprises enzymes involved in translation, ribosome assembly, signal transduction (Ras-like proteins and heterotrimeric G proteins), cell motility and intracellular transport. All GTPases have a conserved G-domain composed of five structural motifs (G1–G5) responsible for binding the guanine nucleotides. This domain undergoes large conformational changes during the functional cycle of the enzyme that alternates from an inactive state bound to GDP to an active state in complex with GTP [20,21]. Such classical GTPases whose structures differ in the apo-form or bound to different nucleotides comprise EF-Tu and

* Corresponding author. Fax: +52 5556162203.
E-mail address: nuriasp@unam.mx (N. Sánchez-Puig).

0006-291X/$ - see front matter © 2013 Elsevier Inc. All rights reserved.
http://dx.doi.org/10.1016/j.bbrc.2013.06.077

p21 Ras [22,23]. However, not all studied GTPases switch conformation upon nucleotide binding, instead this change is triggered by effector biomolecules. These non-canonical GTPases include the translocase EF-G/EF-2 [24]. The functional cycle of a GTPase is better understood in terms of a GTP-favoring conformation and a GDP-favoring conformation rather than GDP- or GTP-bound states [25]. Negative regulators that increase the hydrolysis rate of GTP are designated as GAPs or GTPase-Activating Proteins. For many GTPases involved in translation or ribosome biogenesis, the ribosomal subunits have been shown to be the GAP effector. On the other hand, activating biomolecules that accelerate the exchange of GDP for GTP are known as GDP/GTP Exhange Factors (GEFs). Depending on the step at which a GEF exerts its influence they can be subdivided into two types. The Guanine nucleotide Dissociator Stimulator (GDS) increases the rate of GDP dissociation and the GTP Stabilizing Factors (GSF) that favors GTP binding by shifting the equilibrium of the apo-form of the GTPase from the GDP-conformation towards the GTP-conformation [26].

In this study, we used biophysical techniques to characterize the human and *S. cerevisiae* EFL1 GTPases. Both recombinant proteins were folded as judged by their circular dichroism spectra. Despite both proteins being orthologs, with 40% identity and a similar content of secondary structure, they have very different thermal stabilities. The human protein is highly resistant to thermal denaturation while the yeast protein follows a complex denaturation path best described by two transitions with two-state process. To gain insights into the function of the EFL1 GTPases, we characterized their enzymatic properties in the absence and presence of their corresponding biological partner Sdo1/SBDS. Our results showed that in the presence of the Sdo1/SBDS proteins the K_m of the EFL1 GTPases for GTP decreased twofold while the intrinsic hydrolysis rate was not altered. These results suggest that the Sdo1/SBDS proteins act as nucleotide exchange factors that stabilize binding to GTP for the yeast and human EFL1 GTPases, respectively.

2. Material and methods

2.1. Protein expression and purification

Human SBDS (NP_057122) and *S. cerevisiae* Sdo1 (NP_013122) were recombinantly expressed in *Escherichia coli* C41 and purified as described in [27]. Human EFL1 (NP_078856) and *S. cerevisiae* Efl1 (NP_014236) were recombinantly expressed in *S. cerevisiae* and purified as described in [13]. Briefly, the SBDS/Sdo1 proteins were cloned in the pRSET-A vector (Invitrogen) fused to a *N*-terminal 6 × His-Tag. Protein purification consisted of an initial Ni^{2+} affinity chromatography using a His Trap FF column (GE Healthcare) followed by a cationic exchange chromatography using a HiTrap SP FF column (GE Healthcare). The EFL1 proteins were cloned into de pYES2/CT vector (Invitrogen) and expressed with galactose in *S. cerevisiae* BCY123. Protein purification consisted of a Ni^{2+} affinity chromatography using a His Trap FF column (GE Healthcare) followed by an anionic exchange chromatography using a HiTrap Q Sepharose FF column (GE Healthcare) and a size exclusion chromatography with a HiLoad 16/600 Superdex 200 column (GE Healthcare). Protein purity was assessed by SDS–PAGE and the samples were stored in 50 mM Tris–HCl pH 8.0, 100 mM NaCl, 5 mM $MgCl_2$, 10% glycerol at −80 °C until further use.

2.2. Circular dichroism (CD)

Circular dichroism wavelength scan measurements were followed at 25 °C with a JASCO J-720 spectropolarimeter equipped with a Peltier temperature controller. CD spectra were recorded using a 1 mm cuvette and a protein concentration of 0.05 mg/mL for both human and *S. cerevisiae* EFL1 proteins. Scan wavelength was followed from 260 to 190 nm, with an increase of 0.5 nm per step, an averaging time of 5 s and a bandwith of 1 nm. Spectral data were deconvoluted using the program CDNN [28]. The samples were dialyzed against a buffer containing 25 mM sodium phosphate buffer pH 7.2, 25 mM NaCl. Temperature dependence of ellipticity was followed at 208 nm from 20–90 °C, a bandwidth of 1 nm, a time response of 5 s and a temperature gradient of 1 °C/min. The data was fitted to a Boltzmann distribution describing a standard two-state transition model to obtain the melting temperature.

2.3. Differential scanning calorimetry (DSC)

DSC measurements were performed using a VP-DSC Capillary Cell Microcalorimeter-Autosampler (MicroCal, Inc.). Samples contained a protein concentration between 0.5–1.5 mg/mL and were dialyzed against a buffer consisting of 50 mM Tris–HCl pH 8.0, 300 mM NaCl, 5 mM $MgCl_2$, 10% (v/v) glycerol. Samples and buffer were degassed for 10 min before loading into the calorimetry instrument. Buffer baselines were collected under identical conditions and were subtracted from the corresponding data of the protein samples. A scan rate of 1.5 °C/min was used. Calorimetric enthalpies (ΔH_{cal}) and *T*m values were calculated by integration of the measured heat absorption peaks after subtraction of the buffer baseline. Calorimetric data were adjusted to a model of two transitions with two states for each transition using the software provided by the manufacturer.

2.4. Enzyme kinetics

Hydrolysis of GTP was measured by the MESG/phosphorylase system previously described by Webb [29]. Standard reactions consisted of 150 μL solution containing 50 mM Tris–HCl pH 7.5, 1 mM $MgCl_2$, 0.2 mM MESG, 1.0 U purine nucleoside phosphorylase and the indicated amounts of GTP. Measurements done in the presence of effector protein also contained 10 μM of Sdo1 or SBDS. At this concentration of effector protein more than 98% of the GTPase is bound to it (data not shown). Reactions were initiated by adding a final concentration of 3 μM of the corresponding GTPase. Time courses were followed by recording the change in absorbance at 360 nm in a Cary®50 UV–Vis spectrophotometer (Agilent Technologies). Background absorbance was recorded prior to the addition of the GTPase and subtracted from the sample signals. The phosphorylase coupled reaction is extremely fast, and thus the slope of the measured time course is proportional to the hydrolysis rate of the tested GTPase. The concentration of phosphate ions released in the reaction was estimated considering a molar absorption coefficient at 360 nm of 14,386 M^{-1} cm^{-1} obtained from our experimental standard curve. Kinetic data were analyzed by nonlinear regression to the Michaelis–Menten equation with the program Kaleidagraph 4.1.3 (Synergy Software).

3. Results and discussion

3.1. Secondary structure and stability analysis of the EFL1 GTPases

We studied the structural content of the human and *S. cerevisiae* EFL1 by circular dichroism. This technique is a sensitive spectroscopic method for analyzing the secondary structure and the thermal stability of proteins. The far-UV CD spectra for the human and *S. cerevisiae* EFL1 consisted of the typical signature of mixed secondary structure (negative bands at 222 and 208 nm for α-helices and a negative band at 217 nm for β-sheets). Both spectra had the same overall shape with a pronounced minimum at 208 nm, a less

marked minimum at 222 nm and a positive signal at 200 nm. This suggests that the secondary structure content for both GTPases consist of a mixture of α-helices and β-sheets whose signals mask each other resulting in a plateau rather than the characteristic minima (Fig. 1). Deconvolution of both CD spectra resulted in a secondary structure content of 37% and 34% of α-helix, and 15% and 17% of β-sheet for the yeast and human EFL1 proteins respectively. These values agree well with the secondary structure content obtained from the crystallographic structure of the homolog protein EF-2 (PDB:1N0V) corresponding to 38% of α-helix and 23% of β-sheet. The CD signal of human EFL1 did not change markedly with increasing temperature and lacked any cooperative transition. The linear shape of the spectrum with a slight positive slope and a CD signal of −15,000 degree cm^2 $dmol^{-1}$ obtained at the highest temperature reached in the experiment suggested that unfolding did not occur. The trace obtained from the cooling down experiment, however, did not overlap with that of the heating up suggesting that some secondary structure was lost by the temperature treatment and unfolding was not reversible (Fig. 2A). The same results were obtained when monitoring the thermal denaturation of human EFL1 using differential scanning calorimetry (data not shown). On the other hand, the temperature dependency against the CD signal for the yeast EFL1 described a sigmoidal curve and thus elicited a cooperative denaturation transition. The denaturation process comprised an interval of temperature of 35 °C and it was not reversible (Fig. 2B). Data were fitted to a two-state transition model to obtain the apparent parameters that described the process. The apparent temperature of unfolding of the yeast EFL1 corresponded to 51 °C with an apparent van't Hoff enthalpy of 32.3 kcal mol^{-1}. The CD signal at the end of the process did not reach values close to zero, instead it still consisted of a large value −8000 degree cm^2 $dmol^{-1}$ suggesting that not all the secondary structure was lost even at high temperaures. To validate this assumption, we further monitored the denaturation process using differential scanning calorimetry (Fig. 2C). The DSC trace displayed two transitions, the first one started at a temperature of 38 °C with the second ending close to 75 °C. This denaturation interval (~37 °C) coincided with that previously observed in the circular dichroism experiment. As it happened with the thermal denaturation of yeast EFL1 followed by circular dichroism, the DSC

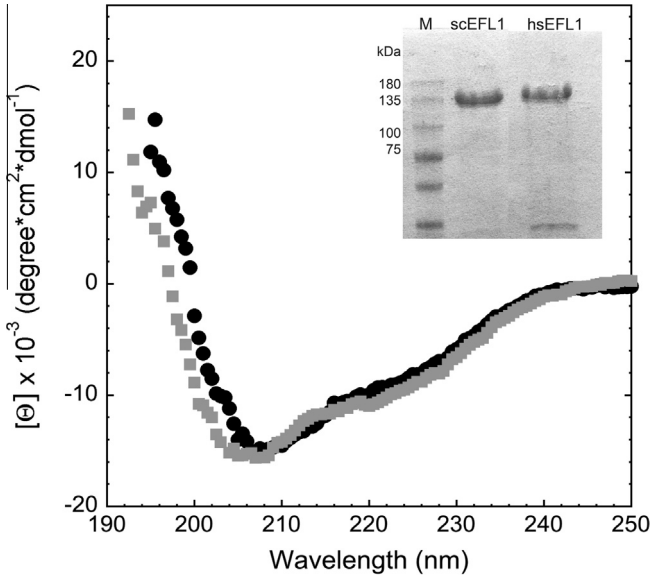

Fig. 1. Far-UV circular dichroism spectra of *S. cerevisiae* EFL1 (black) and human EFL1 (grey). Inset shows an SDS–PAGE of the purified recombinant proteins used in this study. M - Molecular weight marker, sc - *S. cerevisiae*, hs - human.

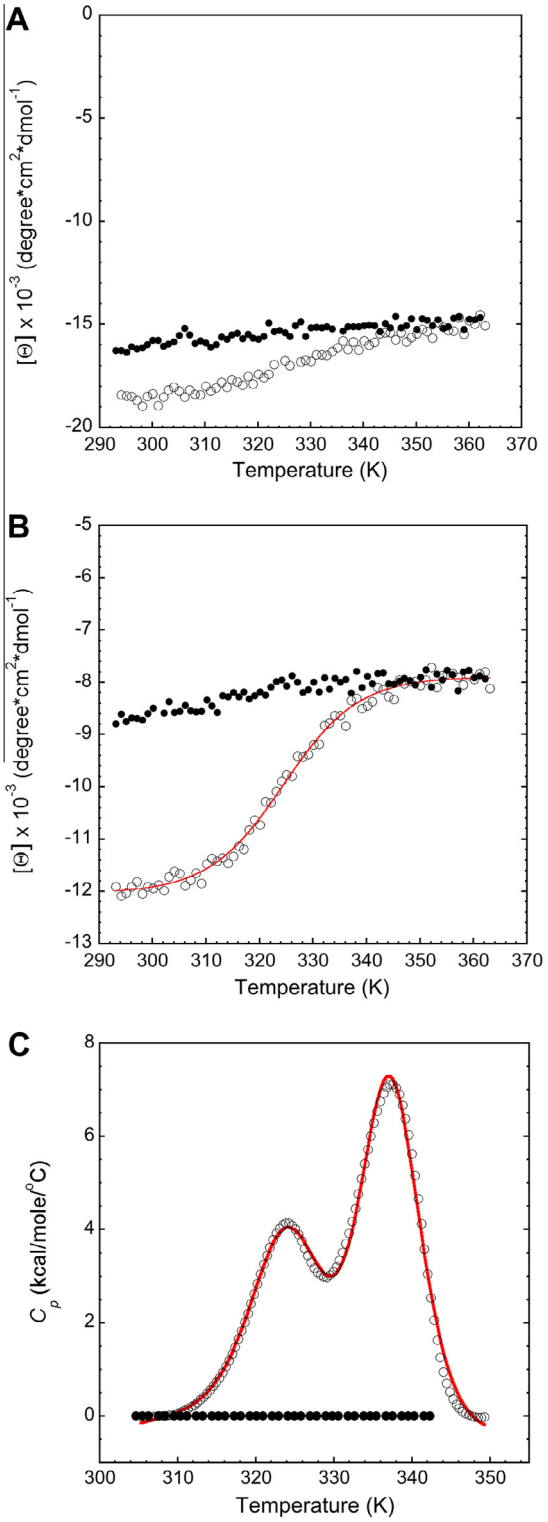

Fig. 2. Thermal stability of *S. cerevisiae* and human EFL1. (A) Temperature dependence of the molar ellipticity of human EFL1. The white trace corresponds to the heating of the sample from 20 to 90 °C and the black trace corresponds to the cooling of the sample after heating. (B) Temperature dependence of the molar ellipticity of *S. cerevisiae* EFL1. The white trace corresponds to the heating of the sample from 20 to 90 °C and the black trace corresponds to the cooling of the sample after heating. Solid line represents the fit to a two-state denaturation process. (C) DSC thermograms of *S. cerevisiae* EFL1 denaturation. The white trace corresponds to the heating of the sample from 20 to 75 °C and the black trace corresponds to the rescan of the sample after heating it. Solid line represents the fit to a two-transition model with two-states for each transition.

experiment showed also an irreversible process. Data best described a two-transition model with two-states for each transition ($N \leftrightarrow I \leftrightarrow U$) and different C_p. The apparent melting temperatures corresponded to 54 and 64 °C for the first and second transition respectively. Interestingly, the average of these two transition temperatures (59 °C) is very close to that observed when fitting the CD data to a two-state model. The apparent calorimetric enthalpies for both transitions corresponded to $\Delta H_{cal1} = 56$ kcal mol^{-1} and $\Delta H_{cal2} = 85$ kcal mol^{-1}. These results suggest a non-two state thermal unfolding behavior for the yeast EFL1. Furthermore, unfolding most likely involves the formation of unfolding intermediates since the van't Hoff enthalpy is smaller than the calorimetric enthalpy ($\Delta H_{vH} = 32$ kcal mol^{-1} < $\Delta H_{cal} = 141$ kcal mol^{-1}). A homology-based model of *S. cerevisiae* EFL1 using the crystallographic structure of EF-2 showed that the EFL1 protein also consists of 5 domains [17]. In this model, the interface between domain III:V is crucial for the conformational changes predicted to occur in EFL1 with domains I–II pointing to one side of the molecule and domain IV to the opposite. This structural organisation with interlocked domains may explain the presence of unfolding intermediates observed for the yeast EFL1.

The results presented in this section demonstrate that human and yeast recombinant EFL1 GTPase are folded and their secondary structure consists of a mixture of α-helices and β-sheets. Despite sharing a similar content of secondary structure and 40% identity, they have very different thermal stabilities. The human EFL1 is highly resistant to thermal denaturation while the yeast protein unfolds in a complex process that involves the presence of unfolding intermediates.

3.2. Kinetic studies of the EFL1 GTPases and the SBDS/Sdo1 effector protein

The MESG/purine phosphorylase assay was used to measure the kinetics of PO_4^{3-} release from GTP hydrolysis by the EFL1 GTPases. Steady-state kinetic analyses in the presence of 1 mM Mg^{2+} revealed slow but saturable kinetics of GTP with the concomitant production of inorganic phosphate (Fig. 3 and Table 1). Activity time courses showed more than 10 turnovers per active site. Values of k_{cat} and K_m were 0.47 min^{-1} and 110 μM for the *S. cerevisiae* EFL1, and 0.27 min^{-1} and 176 μM for the human EFL1. These results suggest that the yeast EFL1 is a slightly better catalytic enzyme than its human counterpart. The steady-state rates of GTP hydrolysis observed for the EFL1 proteins are comparable to those of other ribosomal GTPases such as yeast Nug1 and its bacterial homolog RbgA [8,30]. Compared to some small GTPases that perform single-turnover in the presence of Mg^{2+} and necessarily require the interaction with effector biomolecules to be activated [31], most ribosomal GTPases release GDP spontaneous and may not need a dedicated GEF [5]. The observation of mutiple turn-over reaction for the EFL1 GTPases suggest that release of GDP is spontaneous with a low binding affinity. Indeed, we have evidence that the EFL1 dissociation constants for GDP are in the hundred of micromolar for both the human and the yeast proteins (unpublished results).

As evidenced here and in other reports, ribosomal GTPases are not elated enzymes with k_{cat} values of only 0.1–0.5 min^{-1}. This slow activity does not match the scale of their cellular function, since growing cell contains 200,000 ribosomes synthesized at a rate of 2000 ribosomes per min [32]. However, they are still good catalysts, in particular if we compare their k_{cat} values with the first-order rate constant of the corresponding uncatalyzed reaction in water. The first-order rate enhancement, k_{cat}/k_{uncat}, obtained for both the yeast and human EFL1 GTPases suggest that these enzymes accelerate GTP hydrolysis by 10^5 (Table 1). Previous reports suggested that in the presence of Sdo1/SBDS the corresponding EFL1 protein elicited a net increase in activity [13,15]. These studies, however, did not address at which step of the catalytic pathway the Sdo1/SBDS proteins are exerting its influence. In this work, kinetics of the EFL1 GTPases perfomed in the presence of saturating concentrations of Sdo1 and SBDS showed that k_{cat} values remained unaltered while the K_m was reduced in half for both the yeast and the human EFL1 proteins (Fig. 3 and Table 1). Control experiments done with the Sdo1 and SBDS proteins alone did not show any change in the absorbance at 360 nm suggesting that no hydrolysis had occured (Fig. 3). The change in K_m could only have occured due to a change in the enzymatic properties of the EFL1 GTPases. This change in the K_m suggests that the Sdo1 and SBDS proteins act as guanine exchange factors or GEFs for the *S. cerevisiae* and human EFL1 GTPases respectively. If we consider a three-step reaction mechanism like

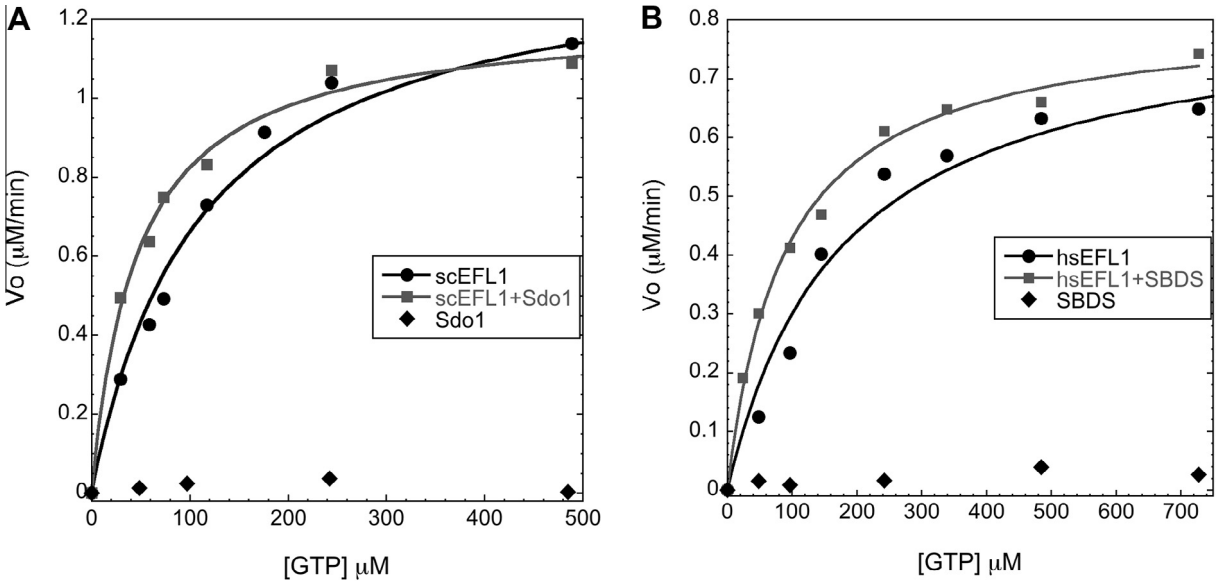

Fig. 3. Determination of the kinetic parameters catalyzed by the *S. cerevisiae* (A) and human EFL1 (B) GTPases. (•) GTPase, (■) GTPase in the presence of effector protein, (♦) effector protein alone. Solid lines represent the fit to the Michaelis–Menten equation.

Table 1
Summary of kinetic data for the activities of the *S. cerevisiae* (sc) and human (hs) EFL1 GTPases on their own and in the presence of their corresponding effector protein.

	V_{max} (μM/min)	K_m (μM)	k_{cat} (min^{-1})	k_{cat}/K_m (M^{-1} s^{-1})	First-order rate enhancement[a] (k_{cat}/k_{uncat})
scEFL1	1.4 ± 0.07	110 ± 16	0.47 ± 0.02	71 ± 11	2×10^5
scEFL1 + Sdo1	1.3 ± 0.05	60 ± 8	0.43 ± 0.02	118 ± 16	1.9×10^5
hsEFL1	0.8 ± 0.06	176 ± 37	0.27 ± 0.02	26 ± 6	1.2×10^5
hsEFL1 + SBDS	0.8 ± 0.03	83 ± 9	0.27 ± 0.01	54 ± 6	1.2×10^5

[a] k_{uncat} is the rate constant for the uncatalyzed hydrolysis of $MgATP^{2-}$ [38], as to date no reports exist for the uncatalyzed hydrolysis of $MgGTP^{2-}$.

the one described below in which release of the inorganic phosphate renders the equilibrium irreversible in one direction

$$E + GTP \underset{k_{-1}}{\overset{k_1}{\rightleftharpoons}} E{\bullet}GTP \underset{PO_4^{-3}}{\overset{k_2}{\rightarrow}} E{\bullet}GDP \underset{k_{-3}}{\overset{k_3}{\rightleftharpoons}} E + GDP$$

and whose kinetic parameters for the forward reaction are defined as follow:

$$k_{cat} = (k_2k_3)/(k_2 + k_3) \quad K_{m(GTP)} = (k_{-1}k_3) + (k_2k_3)/k_{-1}(k_2 + k_3) \quad [33]$$

shows that the only microscopic rate constant that can be modified due to the prescence of Sdo1/SBDS is k_{-1}. The quotient of k_{-1} and k_1 describes the dissociation constant for GTP binding. Thus, a decrease in the K_m values (with no change in k_{cat}) mediated by the Sdo1 and SBDS proteins suggest that they are GEFs specifically functioning as guanine stabilizing factors or GSFs for the EFL1 GTPases. The only GSF modulator described for a ribosomal GTPase is Rcl1 for Bms1 [7]. The list of GSF modulators for translation GTPases is more extense. Aminoacyl-tRNA acts as a GSF for EF-Tu/eEF1A [34] just as initiator tRNA serves for aIF2 [35] and the pretranslocation complex is for EF-G [36]. Coincidentally, it has been proposed that the shape of the SBDS protein resembles that of a tRNA [27,37] and EFL1 may function analogously to EF-G/tRNA in a translocation-like step to release SBDS and eIF6 (Tif6).

Steady-state enzyme kinetics demonstrated that the yeast and human EFL1 GTPases are capable of multiple turnovers. Characterization of the kinetic parameters of these GTPases in the presence of their corresponding effector proteins, Sdo1 and SBDS, suggests that the latter act as nucleotide exchange factors stabilizing the binding of GTP to EFL1.

Acknowledgments

The authors thank Dr. Luis F. Olguín (Facultad de Química, UNAM) for helpful comments on this manuscript. One of the authors (N. S-P) acknowledges the financial support from DGAPA-UNAM project PAPIIT No. 204010 and CONACYT (México) Project No. 167359.

References

[1] M. Fromont-Racine, B. Senger, C. Saveanu, F. Fasiolo, Ribosome assembly in eukaryotes, Gene 313 (2003) 17–42.
[2] H. Tschochner, E. Hurt, Pre-ribosomes on the road from the nucleolus to the cytoplasm, Trends Cell Biol. 13 (2003) 255–263.
[3] A.K. Henras, J. Soudet, M. Gerus, S. Lebaron, M. Caizergues-Ferrer, A. Mougin, Y. Henry, The post-transcriptional steps of eukaryotic ribosome biogenesis, Cell. Mol. Life Sci. 65 (2008) 2334–2359.
[4] B.S. Strunk, K. Karbstein, Powering through ribosome assembly, RNA 15 (2009) 2083–2104.
[5] K. Karbstein, Role of GTPases in ribosome assembly, Biopolymers 87 (2007) 1–11.
[6] R.A. Britton, Role of GTPases in bacterial ribosome assembly, Annu. Rev. Microbiol. 63 (2009) 155–176.
[7] K. Karbstein, S. Jonas, J.A. Doudna, An essential GTPase promotes assembly of preribosomal RNA processing complexes, Mol. Cell 20 (2005) 633–643.
[8] J. Bassler, M. Kallas, E. Hurt, The NUG1 GTPase reveals and *N*-terminal RNA-binding domain that is essential for association with 60S pre-ribosomal particles, J. Biol. Chem. 281 (2006) 24737–24744.
[9] J. Hedges, M. West, A.W. Johnson, Release of the export adapter, Nmd3p, from the 60S ribosomal subunit requires Rpl10p and the cytoplasmic GTPase Lsg1p, EMBO J. 24 (2005) 567–579.
[10] B.C. Jensen, Q. Wang, C.T. Kifer, M. Parsons, The NOG1 GTP-binding protein is required for biogenesis of the 60S ribosomal subunit, J. Biol. Chem. 278 (2003) 32204–32211.
[11] T.F. Menne, B. Goyenechea, N. Sanchez-Puig, C.C. Wong, L.M. Tonkin, P.J. Ancliff, R.L. Brost, M. Costanzo, C. Boone, A.J. Warren, The Shwachman–Bodian–Diamond syndrome protein mediates translational activation of ribosomes in yeast, Nat. Genet. 39 (2007) 486–495.
[12] C. Saveanu, D. Bienvenu, A. Namane, P.E. Gleizes, N. Gas, A. Jacquier, M. Fromont-Racine, Nog2p, a putative GTPase associated with pre-60S subunits and required for late 60S maturation steps, EMBO J. 20 (2001) 6475–6484.
[13] A.J. Finch, C. Hilcenko, N. Basse, L.F. Drynan, B. Goyenechea, T.F. Menne, A. Gonzalez Fernandez, P. Simpson, C.S. D'Santos, M.J. Arends, J. Donadieu, C. Bellanne-Chantelot, M. Costanzo, C. Boone, A.N. McKenzie, S.M. Freund, A.J. Warren, Uncoupling of GTP hydrolysis from eIF6 release on the ribosome causes Shwachman–Diamond syndrome, Genes Dev. 25 (2011) 917–929.
[14] S. Klinge, F. Voigts-Hoffmann, M. Leibundgut, S. Arpagaus, N. Ban, Crystal structure of the eukaryotic 60S ribosomal subunit in complex with initiation factor 6, Science 334 (2011) 941–948.
[15] B. Senger, D.L. Lafontaine, J.S. Graindorge, O. Gadal, A. Camasses, A. Sanni, J.M. Garnier, M. Breitenbach, E. Hurt, F. Fasiolo, The nucle(ol)ar Tif6p and Efl1p are required for a late cytoplasmic step of ribosome synthesis, Mol. Cell 8 (2001) 1363–1373.
[16] J.S. Graindorge, J.C. Rousselle, B. Senger, P. Lenormand, A. Namane, F. Lacroute, F. Fasiolo, Deletion of EFL1 results in heterogeneity of the 60S GTPase-associated rRNA conformation, J. Mol. Biol. 352 (2005) 355–369.
[17] C. Bussiere, Y. Hashem, S. Arora, J. Frank, A.W. Johnson, Integrity of the P-site is probed during maturation of the 60S ribosomal subunit, J. Cell Biol. 197 (2012) 747–759.
[18] K.Y. Lo, Z. Li, C. Bussiere, S. Bresson, E.M. Marcotte, A.W. Johnson, Defining the pathway of cytoplasmic maturation of the 60S ribosomal subunit, Mol. Cell 39 (2010) 196–208.
[19] D.D. Leipe, Y.I. Wolf, E.V. Koonin, L. Aravind, Classification and evolution of P-loop GTPases and related ATPases, J. Mol. Biol. 317 (2002) 41–72.
[20] H.R. Bourne, D.A. Sanders, F. McCormick, The GTPase superfamily: conserved structure and molecular mechanism, Nature 349 (1991) 117–127.
[21] I.R. Vetter, A. Wittinghofer, The guanine nucleotide-binding switch in three dimensions, Science 294 (2001) 1299–1304.
[22] H. Berchtold, L. Reshetnikova, C.O. Reiser, N.K. Schirmer, M. Sprinzl, R. Hilgenfeld, Crystal structure of active elongation factor Tu reveals major domain rearrangements, Nature 365 (1993) 126–132.
[23] E.F. Pai, U. Krengel, G.A. Petsko, R.S. Goody, W. Kabsch, A. Wittinghofer, Refined crystal structure of the triphosphate conformation of H-ras p21 at 1.35 Å resolution: implications for the mechanism of GTP hydrolysis, EMBO J. 9 (1990) 2351–2359.
[24] R. Jorgensen, P.A. Ortiz, A. Carr-Schmid, P. Nissen, T.G. Kinzy, G.R. Andersen, Two crystal structures demonstrate large conformational changes in the eukaryotic ribosomal translocase, Nat. Struct. Biol. 10 (2003) 379–385.
[25] V. Hauryliuk, S. Hansson, M. Ehrenberg, Cofactor dependent conformational switching of GTPases, Biophys. J. 95 (2008) 1704–1715.
[26] J. Cherfils, M. Zeghouf, Regulation of small GTPases by GEFs, GAPs, and GDIs, Physiol. Rev. 93 (2013) 269–309.
[27] C. Shammas, T.F. Menne, C. Hilcenko, S.R. Michell, B. Goyenechea, G.R. Boocock, P.R. Durie, J.M. Rommens, A.J. Warren, Structural and mutational analysis of the SBDS protein family. Insight into the leukemia-associated Shwachman–Diamond Syndrome, J. Biol. Chem. 280 (2005) 19221–19229.
[28] G. Bohm, R. Muhr, R. Jaenicke, Quantitative analysis of protein far UV circular dichroism spectra by neural networks, Protein Eng. 5 (1992) 191–195.
[29] M.R. Webb, A continuous spectrophotometric assay for inorganic phosphate and for measuring phosphate release kinetics in biological systems, Proc. Natl. Acad. Sci. USA 89 (1992) 4884–4887.
[30] D. Achila, M. Gulati, N. Jain, R.A. Britton, Biochemical characterization of ribosome assembly GTPase RbgA in *Bacillus subtilis*, J. Biol. Chem. 287 (2012) 8417–8423.
[31] B. Zhang, Z.X. Wang, Y. Zheng, Characterization of the interactions between the small GTPase Cdc42 and its GTPase-activating proteins and putative effectors.

Comparison of kinetic properties of Cdc42 binding to the Cdc42-interactive domains, J. Biol. Chem. 272 (1997) 21999–22007.
[32] J.R. Warner, The economics of ribosome biosynthesis in yeast, Trends Biochem. Sci. 24 (1999) 437–440.
[33] A. Cornish-Bowden, Introduction to Enzyme Kinetics, Portland Press, London, 1995.
[34] V.A. Dell, D.L. Miller, A.E. Johnson, Effects of nucleotide- and aurodox-induced changes in elongation factor Tu conformation upon its interactions with aminoacyl transfer RNA. A fluorescence study, Biochemistry 29 (1990) 1757–1763.
[35] L. Yatime, Y. Mechulam, S. Blanquet, E. Schmitt, Structural switch of the gamma subunit in an archaeal aIF2 alpha gamma heterodimer, Structure 14 (2006) 119–128.
[36] B. Wilden, A. Savelsbergh, M.V. Rodnina, W. Wintermeyer, Role and timing of GTP binding and hydrolysis during EF-G-dependent tRNA translocation on the ribosome, Proc. Natl. Acad. Sci. USA 103 (2006) 13670–13675.
[37] A. Savchenko, N. Krogan, J.R. Cort, E. Evdokimova, J.M. Lew, A.A. Yee, L. Sanchez-Pulido, M.A. Andrade, A. Bochkarev, J.D. Watson, M.A. Kennedy, J. Greenblatt, T. Hughes, C.H. Arrowsmith, J.M. Rommens, A.M. Edwards, The Shwachman–Bodian–Diamond syndrome protein family is involved in RNA metabolism, J. Biol. Chem. 280 (2005) 19213–19220.
[38] R.B. Stockbridge, R. Wolfenden, The intrinsic reactivity of ATP and the catalytic proficiencies of kinases acting on glucose, *N*-acetylgalactosamine, and homoserine: a thermodynamic analysis, J. Biol. Chem. 284 (2009) 22747–22757.